Available online at www.sciencedirect.com
ScienceDirect
Lithos 97 (2007) 161–173
LITHOS
www.elsevier.com/locate/lithos

He, Pb and S isotopic constraints on the relationship between the A-type Qitianling granite and the Furong tin deposit, Hunan Province, China

Zhao-li Li [a,b], Rui-zhong Hu [a,*], Jing-sui Yang [b], Jian-tang Peng [a], Xiao-min Li [a], Xian-wu Bi [a]

[a] State Key Laboratory of Ore Deposit Geochemistry, Institute of Geochemistry, Chinese Academy of Sciences, Guiyang 550002, China
[b] Key Laboratory of Continental Dynamics, Institute of Geology, Chinese Academy of Geological Science, Beijing 100037, China

Received 31 October 2005; accepted 4 December 2006
Available online 15 December 2006

Abstract

The Furong tin deposit, located in southern Hunan Province, China, is a large, newly discovered deposit with an estimated Sn reserve of about 700,000 tons. The deposit is spatially and temporally associated with the A-type Qitianling granite. The $^{3}He/^{4}He$ ratios of fluid inclusions trapped in sulfides from the deposit range from 0.13 to 2.95 Ra, indicating a mixed crust-mantle source, similar to that of the Qitianling granite complex. Lead isotopes in feldspars of the granite (mostly in the range of $^{206}Pb/^{204}Pb = 18.547–19.180$, $^{207}Pb/^{204}Pb = 15.598–15.825$, $^{208}Pb/^{204}Pb = 37.912–39.068$) and in sulfide minerals ($^{206}Pb/^{204}Pb = 18.467–18.836$, $^{207}Pb/^{204}Pb = 15.503–15.772$, $^{208}Pb/^{204}Pb = 38.607–39.099$) are essentially the same, indicating that the lead in both was derived mainly from the upper crust, with a small mantle component. The sulfur isotopic values of the ore minerals vary widely, ranging from −26.1‰ to +10.4‰, but are mainly within the range of +0.2‰ to +10.4‰, implying that the S in the hydrothermal fluids was derived mainly from magmatic fluids, with minor contributions from the mantle, sedimentary rocks and biogenic material. The He, Pb and S isotopes all confirm that the ore-forming fluids of the Furong deposit were magmatic in origin, derived from the melts that produced the Qitianling A-type granite. The tin mineralization occurs within, or along the margins of, the Qitianling granite complex, and the timing of the mineralization coincides with the intrusive age of the granite. The available data suggest that the emplacement of the granites and the mineralization was related to mantle upwelling and extension of the lithosphere in South China during the Mesozoic.

Keywords: He, Pb and S isotopes; Furong tin deposit; A-type granite; Qitianling granite complex

1. Introduction

Typical $^{3}He/^{4}He$ ratios of crustal rocks are 0.01–0.05 Ra (Stuart et al., 1995), whereas those of the mantle are 6–7 Ra (Dunaim and Baur, 1995). This vast difference in isotopic ratios (a factor of 1000) makes it possible to use He isotopes to monitor processes by which mantle volatiles are added to crustal rocks and to trace the origins of ore-forming fluids (Simmons et al., 1987; Stuart et al., 1995; Hu et al., 1998; Burnard et al., 1999; Kendrick et al., 2001; Yamamoto et al., 2001; Ballentine et al., 2002; Kendrick et al., 2002; Zhao et al., 2002; Burnard and Polya, 2004).

* Corresponding author.
E-mail addresses: lizhaoli3@tom.com (Z. Li), huruizhong@vip.163.com (R. Hu).

0024-4937/$ - see front matter © 2006 Elsevier B.V. All rights reserved.
doi:10.1016/j.lithos.2006.12.009

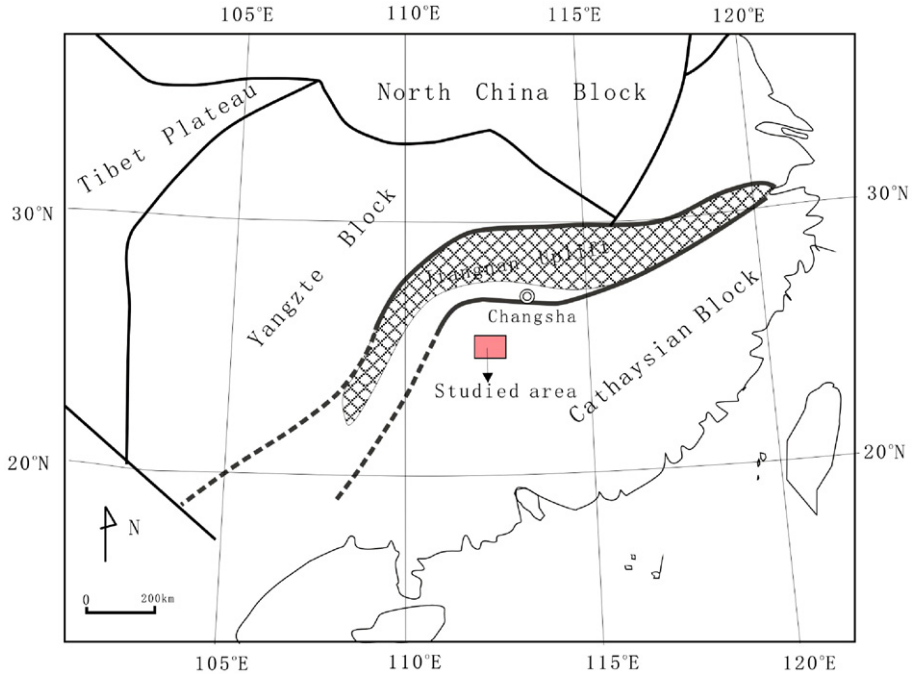

Fig. 1. Geological sketch map of South China.

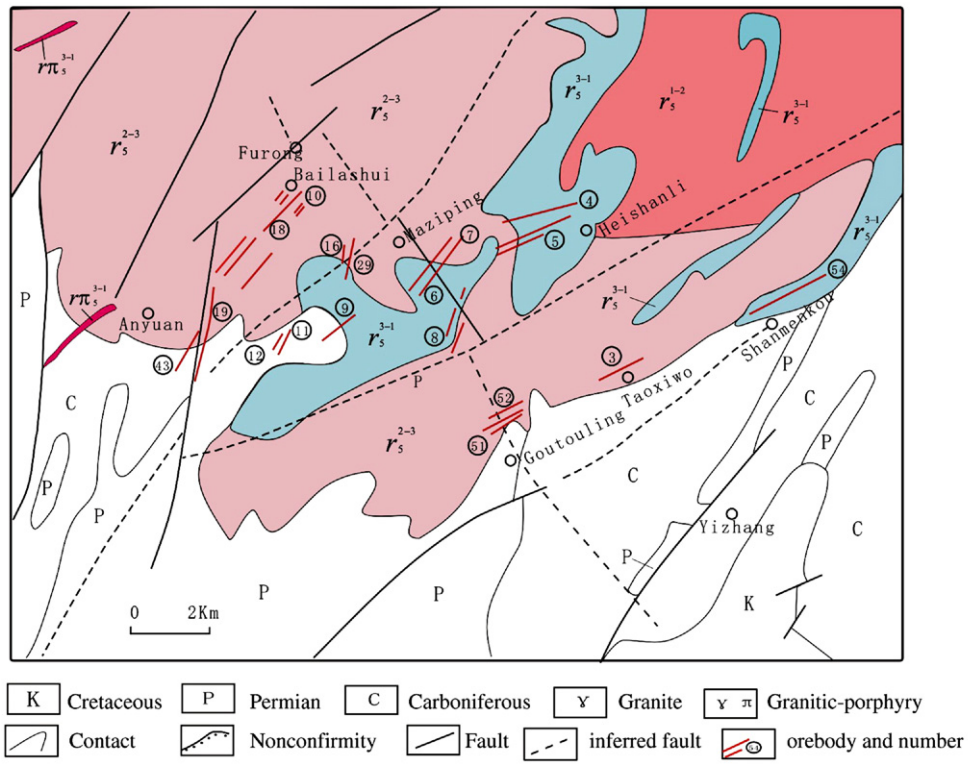

Fig. 2. Geological sketch map of the Furong tin deposit (after South Hunan Institute of Mineral Resources and Survey, 2002).

A review of global tin deposits by Janecka and Stemprok (1967) showed that 82% of the deposits are genetically associated with granites, particularly with Mesozoic or Cenozoic granites (Chen and Mao, 1995). Later studies documented that tin deposits are mostly associated with S-type granites, but recently a number of deposits have been shown to be genetically related to A-type granites. Examples of such occurrences are found in South Africa (Robb et al., 1994), Brazil (Nilson and Márcia, 1998; Lenharo et al., 2003), southeastern Fennoscandia (Haapala, 1995), Missouri, USA (Sawkins, 1984), China (Bi et al., 1992; Liu et al., 1997; Qu et al., 2002) and Nigeria (Sawkins, 1984; Taylor, 1979). Helium isotopes have not been previously used to study the genetic relations between tin deposits and A-type granites.

Tin deposits associated with the A-type granites formed mainly in extensional regimes in continental lithosphere, unlike those associated with S-type granites. However, little is known about the processes by which these deposits are formed. As part of an ongoing effort to characterize such deposits, this paper reports He, S and Pb isotopic compositions of a large, newly discovered tin deposit — the Furong deposit in Hunan Province, China. Isotope data on the deposit and its host granites may provide a better understanding of the origin of such deposits. Thus far, only basic petrological and mineralogical data have been published on the Furong tin ore deposit (Zheng and Jia, 2001; Zhu et al., 2003; Wang et al., 2004; Cai et al., 2004; Zheng et al., 2005), and neither the source of the ore-forming fluids nor their relationship to the granites is well understood. In this paper, we discuss the relationship between the A-type Qitianling granite complex and the Furong tin deposit in the light of the He, S and Pb isotopic data.

Table 1
Chemical compositions of the Qitianling granite (wt.%)

Unit	Lijiadong	Wuliqiao	Nanxi	
Sample	Qt-6	Qt-7	Qt-8	Qt-9
SiO_2	68.88	68.47	70.14	70.94
TiO_2	0.56	0.68	0.49	0.42
Al_2O_3	13.88	13.43	13.41	13.19
Fe_2O_3	0.16	0.27	0.26	0.14
FeO	4.02	4.82	4.35	3.86
MnO	0.07	0.06	0.07	0.05
MgO	0.68	0.80	0.57	0.45
CaO	2.02	2.00	2.00	1.67
Na_2O	3.31	2.98	3.37	3.09
K_2O	5.24	5.12	4.59	4.90
P_2O_5	–	–	–	–
Cl	0.02	0.02	0.03	0.05
F	0.12	0.31	0.20	0.18
Total	98.96	98.96	99.48	98.94

Data from Wang et al. (2004).

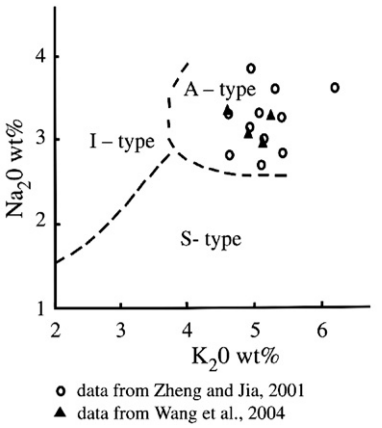

Fig. 3. Na_2O–K_2O diagram of the Qitianling granites (Collins et al., 1982).

2. Geological background and the petrological and geochemical characteristics of the Qitianling granite complex

2.1. Geological background

South China consists of the Yangtze Block to the northwest and the Cathaysian Block to the southeast (Fig. 1). The Yangtze Block is bordered to the north by the North China Block and to the west by the Tibetan Plateau. The Cathaysian Block is composed of a metamorphic basement overlain by a sedimentary cover of folded Late Paleozoic and Cenozoic strata (Huang, 1960). Tectonically, the study area is located in the Cathaysian Block.

The Qitianling granite complex is located in southern part of Hunan Province, where it is cut by a set of faults (Fig. 2). Numerous small faults and folds are also present in the district. The granite complex crops out over an area of about 520 km^2 and ranges in age from Carboniferous to Early Triassic. Two major units, the Cailing and Furong, are recognized in the complex; the Furong unit crops out over an area greater than 400 km^2, and includes six subunits, whereas the Cailing unit is a single body with a surface area of about 120 km^2. Many non-ferrous metal and rare-metal deposits occur in the Qitianling complex and along its contacts (Wei et al., 2002). The Furong tin deposit, which lies in the famous Chenzhou–Lanshan NE-trending W–Sn–Pb–Zn mineralization belt, occurs in the southern part of the complex, about 200 km south of the Changsha (Fig. 1), the capital of Hunan Province.

Table 2
REE and trace elements of the Qitianling granite (ppm)

Unit			Wuliqiao							Lijiadong						Jiangjunzhai		
Sample	FR0	FR1	FR3	FR19-1-1	FR19-41	FR19-42-3	FR19-31	FR19-12	FR19-13	ZK806-2	ZK806-4	ZK804-2	ZK804-3	FR43-4	SMK54-1	TXW3-3	GTL55-1	GTL55-7
La	79.54	43.66	51.22	52.15	58.94	32.68	52.41	82.2	55	85.43	79.66	68.57	89.06	56.55	48.41	46.45	45.49	23.74
Ce	153.17	93.02	103.66	107.91	127.49	69.06	106.85	134.92	109.03	156.17	150.34	139.34	163.76	110.59	96.23	90.08	97.08	51.57
Pr	16.48	10.54	11.28	11.95	14.84	7.75	11.9	14.4	11.41	15.36	14.65	14.97	19.03	11.8	9.97	9.32	10.24	5.62
Nd	57.37	39.12	42.04	46.03	56.07	30.07	43.66	45.81	40.05	48.58	47.42	54.18	65.49	41.5	34.3	33.06	35.26	19.7
Sm	10.05	8.09	8.13	8.76	11.07	5.99	8.14	7.49	7.46	7.76	7.58	9.74	11.2	7.5	7.37	7.1	7.64	4.51
Eu	1.3	1.42	1.15	1.63	1.66	0.98	1.55	0.91	1.13	1	0.95	1.46	1.44	1.17	0.71	1	0.37	0.34
Gd	9.06	7.38	7.58	7.92	10.36	5.2	8.02	6.8	6.67	6.96	7.13	8.72	10.21	7.17	7.34	7.02	7.56	4.47
Tb	1.28	1.13	1.17	1.19	1.53	0.7	1.14	0.94	0.97	1.01	0.96	1.16	1.38	1.04	1.21	1.19	1.27	0.76
Dy	7.04	6.45	6.56	6.46	8.26	3.59	6.72	4.96	5.65	5.31	5.62	6.3	7.69	5.89	7.41	6.83	8.24	4.86
Ho	1.47	1.42	1.36	1.34	1.69	0.77	1.401.12	1.25	1.95	1.21	1.2	1.32	1.58	1.18	1.54	1.53	1.82	1.07
Er	4.16	3.75	3.74	3.6	4.54	1.85	3.9	3.14	3.33	3.37	3.37	3.68	4.33	3.41	4.48	4.42	5.37	3.32
Tm	0.62	0.61	0.58	0.52	0.67	0.28	0.56	0.47	0.53	0.49	0.52	0.59	0.63	0.51	0.7	0.67	0.86	0.51
Yb	3.94	3.96	3.81	3.41	4.27	1.68	3.84	3.15	3.41	3.62	3.41	3.43	4.02	3.33	4.61	4.5	6.09	3.49
Lu	0.56	0.6	0.54	0.5	0.62	0.22	0.53	0.48	0.5	0.54	0.53	0.54	0.58	0.5	0.68	0.61	0.91	0.52
Y	41.2	39.43	40.19	38.79	48.38	19.75	40.06	32.45	36.36	34.72	36.79	39.16	44.76	35.3	46.83	44.21	53.34	34.34
∑REE	346.04	221.15	242.82	253.37	302.01	160.82	250.61	306.79	246.39	336.81	323.34	314	380.4	252.14	224.96	213.78	228.2	124.48
Li	77.23	73.31	75.94	77.03	36.17	135.59	64.62	41.11	30.41	97.4	79.06	92.48	70.47	112.42	72.33	64.97	167.99	48.97
Cs	50.88	44.63	27.91	18.81	13.81	26.66	48.78	18.11	17.93	33.92	31.15	37.61	27.74	37.35	21.4	19.1	27.08	20
Ba	585.28	719.89	519.96	536.92	706.11	454.76	649.52	277.46	554.4	310.22	379.36	809.9	530.23	451.35	340.48	512.32	78.87	194.06
Rb	406.57	319.33	301.01	271.38	318.73	447.31	341.5	317.04	372.26	409.14	567.24	535.87	280.22	340.63	470.01	372.19	461.12	474.96
Sr	163.59	196.91	157.89	254.16	271.01	68.52	230.7	146.88	159.59	203.17	46.19	120.99	192.53	165.81	103.44	117.56	42.35	49.87
Zr	423.82	240.9	328.3	267.15	265.41	118.72	279.75	256.99	294.11	278.96	183.66	169.63	234.52	216.41	125.21	160.83	126.6	95.06
Hf	11.28	7.29	9.42	7.34	7.21	3.19	8.03	7.86	8.25	8.62	5.67	5.02	6.92	6.29	4.4	5.68	5.69	4.32
Nb	31.09	26.51	26.22	28.69	34.85	13.7	28.85	18.55	21.19	20.98	18.48	22.08	25.58	22.79	27.94	24.95	24.91	18.01
Ta	2.51	2.75	2.49	2.34	3.02	1.14	2.84	2.02	2.29	2.16	1.89	1.92	2.35	2.49	3.46	3.35	4.24	2.41
Th	43.76	36.98	49.01	23.83	28.18	22.95	42.12	64.11	47.14	64.71	64.79	33.96	45.85	50.22	57.4	46.92	66.82	61.13
U	12.25	16.18	13.55	7.8	9.86	5.54	13.2	17.1	14.84	18.02	19.62	10.37	14.44	15.67	22.55	19.96	31.6	28.03
Ga	22.23	22.97	20.57	22.68	20.88	30.03	21.7	18.61	18.96	21.72	23.16	21.57	21.73	18.82	20.99	20.61	20.83	18.73
TiO_2(%)	0.62	0.53	0.56	1	0.96	0.36	0.78	0.45	0.5	0.46	0.39	0.6	0.68	0.57	0.28	0.33	0.14	0.1
Sn	72.11	23.21	7.97	115.43	60.24	60.3	43.63	10.32	11	14.7	10.86	41.58	31.56	20	15.62	10.69	14.31	12.35
Zn	74.24	41.76	66.54	80.94	94.6	90.94	74.22	53.44	59.89	39.61	47.32	135.6	69.33	54.44	58.39	35.74	26.87	420.63
Sc	7.3	6.61	6.08	10.25	9.94	4.07	7.83	5.64	5.57	4.9	4.2	6.8	8.47	6.68	4.04	4.18	3.63	2.3

N.B. Samples were analyzed by ICP-MS at the Institute of Geochemistry, Chinese Academy of Sciences, Guiyang, China.

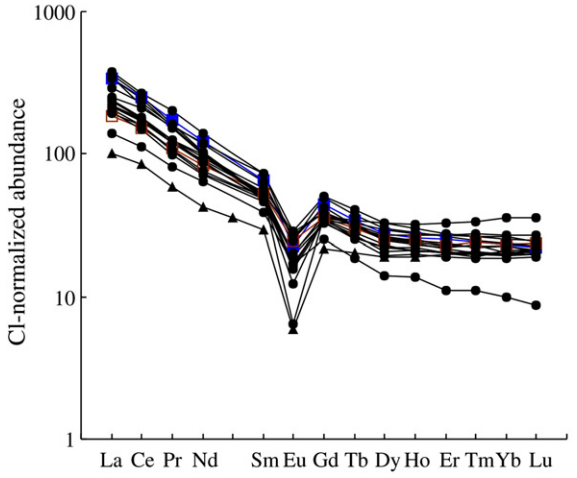

Fig. 4. Chondrite-normalized REE patterns of the Qitianling granites (Sun and McDonough, 1989).

The Furong deposit includes, from NW to SE, the Bailashui–Anyuan, Heishanli–Maziping and Shanmenkou–Taoxiwo–Goutouling NE-trending ore zones (Fig. 2). The granitic rocks in these zones consist mainly of medium-grained, porphyritic hornblende-biotite adamellite and fine- to coarse-grained, porphyritic biotite moyite. The Bailashui ore zone is located in the inner contact zone of the medium-grained adamellite in the southwestern part of the Furong deposit. Twenty-five tin ore veins occur in this zone, the largest of which is Vein 19 (Fig. 2). About 90% of the tin resources in the Furong deposit are concentrated in this zone. Ore veins in the Shanmenkou and Taoxiwo zones are of the greisen type, and they occur in the inner contact zone of the granites; those in the Goutouling zone are of the skarn type, and occur near the granites (Huang et al., 2001).

The ^{40}Ar–^{39}Ar isotopic ages of the granites associated with the ores are mainly of 151–160 Ma (Liu et al., 2003) and recent studies suggest that the main period of mineralization occurred between 150 and 160 Ma (Mao et al., 2004). The main ore mineral is cassiterite, with subordinate pyrite, chalcopyrite, magnetite, galena, sphalerite, and arsenopyrite. Supracrustal rocks in the area are Carboniferous and Permian in age, and the ore veins are hosted mainly in Carboniferous sedimentary rocks of the Shidengzi Group (C_1s) and Permian Qixia Group (P_1q).

2.2. Petrological and geochemical characteristics of the Qitianling granite complex

The Qitianling complex consists chiefly of alkaline, H_2O-undersaturated granitic rocks characterized by high K_2O+Na_2O and SiO_2 contents (Table 1) and strong enrichment in Rb, Th, and large ion lithophile elements (LILE). These features, together with low $^{87}Sr/^{86}Sr$ ratios (Cai et al., 2004), suggest that the Qitianling complex consists of A-type granite (Fig. 3). Rare earth element (REE) concentrations are rather high, (124.48–380.40 ppm; average=262.67 ppm), and on chrondrite-normalized diagrams they display strong LREE enriched and relatively flat HREE patterns (Table 2 and Fig. 4). In addition, the granite is obviously rich in large lithophile elements, especially Rb and Th, but poor in Ba, Nb, Ta, Sr, Eu and Ti (Table 2), implying that the granite may have been derived from crustal melts. Large-scale granitic magmatism occurred in East China from about 160 to 100 Ma as a result of subduction of the lithosphere and upwelling of the asthenosphere (Deng et al., 2004). Thus, the Qitianling granite and associated Furong tin deposit may have formed by crustal melting triggered by heat from the upwelling mantle. This conclusion is supported by the REE and trace element compositions of the granite, which indicate it is an A2-type body (Fig. 5), derived from continental crust.

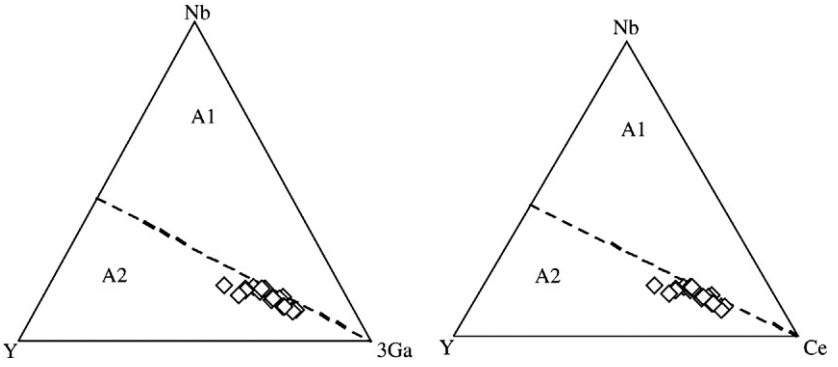

Fig. 5. Y–Nb–Ce and Y–Nb–3Ga diagrams of the Qitianling granites (Eby, 1992).

3. Sampling and analytical procedures

Samples were collected from four representative granitic subunits of the Furong body and four representative ore zones. Two samples of wall rock were also collected. The samples were crushed and the minerals were handpicked under a binocular microscope. The helium isotopic compositions of fluid inclusions and the sulfur isotopic composition of host sulfides, as well as the lead isotopic composition of feldspars and sulfides were measured to constrain the source of the ore-forming fluids and to test for a relationship between the granite complex and the Furong deposit.

The helium isotopic compositions of fluid inclusions in 13 sulfide samples were analyzed on a noble gas mass spectrometer (MI 1201 IG) using the crushing analytical technique at the Stable Isotope Laboratory of the Institute of Resources, Chinese Academy of Geological Sciences, Beijing. The He blank is dominated by diffusion of atmospheric He into the vacuum system. Gas abundances were measured by peak-height comparison with known amounts of air and are accurate to ±5% for ^{4}He measured on a Faraday cup. He blanks are below 0.2 ncc STP ^{4}He, and ^{3}He/^{4}He ratios are accurate to ±5%. All analyses have been corrected for blank values. Details of the analytical procedure are described by Mao et al. (1997) and Li et al. (2002).

The lead isotopic compositions of 22 rock samples and 29 sulfide samples were analyzed on a MAT 261 mass spectrometer using the thermal ionization cross-section analytical technique at the Geological Analysis Laboratory under the Ministry of Nuclear Industry, China. The precision of the ^{208}Pb/^{206}Pb measurements (1 μg of Pb) is ≤0.005%, and the measured ratios (2σ) of international standard sample NBS981 are ^{208}Pb/^{206}Pb = 2.1652465 ± 0.000069, ^{207}Pb/^{206}Pb = 0.9145100 ± 0.000059, and ^{204}Pb/^{206}Pb = 0.059199 ± 0.000013.

The sulfur isotopic compositions of 49 sulfide samples were analyzed on a MAT 251E gas mass spectrometer by using Cu_2O to oxidize the sulfides at the Stable Isotope Laboratory of the Institute of Resources, Chinese Academy of Geological Sciences. The analytical procedure usually yielded an in-run precision of 0.2‰. The calibrations were performed with regular analyses of internal $\delta^{34}S_{CDT}$ standard samples.

4. Results

The He isotopic ratios and abundance data for the analysed samples are given in Table 3. The ^{3}He/^{4}He ratios of fluid inclusions in sulfides from the Furong deposit range from 0.13 to 2.95 Ra, and vary from ore zone to ore zone. Ratios are relatively constant in the fluid inclusions from the Goutouling and Taoxiwo zones, whereas those of the Bailashui ore zone show the full range of variation from 0.13 to 2.95 Ra. In addition, ratios from the Bailashui zone are consistently higher than those from the Taoxiwo zone, and, except for samples FR-19-14, FR-19-15 and FR-19-44, higher than those from the Goutouling zone.

The data listed in Table 4 show that the sulfides are very homogeneous in their Pb isotopic composition; ^{206}Pb/^{204}Pb = 18.547–19.180 (except sample FR2-10-5), ^{207}Pb/^{204}Pb = 15.598–15.825, and ^{208}Pb/^{204}Pb = 37.912–39.068 (except sample FR2-10-1). The data also show that the Pb isotopic composition of the feldspars is similar to that of the sulfides, with values of ^{206}Pb/^{204}Pb = 18.467–18.836, ^{207}Pb/^{204}Pb = 15.503–15.772, and

Table 3
He isotopic compositions of fluid inclusions in sulfides from the Furong tin deposit

Zone	Sample No.	Mineral	^{3}He	^{4}He1	^{3}He/^{4}He	Rc/Ra [a]
			10^{-12} cm^{3}STP/g	10^{-6} cm^{3}STP/g	10^{-7}	
Bailashui	FR19-14	Pyrite	1.74	9.58	1.82±0.57	0.13±0.04
	FR19-15	Pyrite	1.63	8.53	1.91±0.92	0.14±0.07
	FR1-22	Pyrite	21.67	5.82	37.23±4.65	2.68±0.33
	FR19-24	Pyrite	21.31	12.76	16.70±2.00	1.20±0.14
	FR19-35	Arsenopyrite	18.53	4.52	41.00±4.30	2.95±0.31
	FR19-43	Pyrite	9.33	11.96	7.80±1.50	0.56±0.11
	FR19-44	Pyrite	4.74	20.99	2.26±0.36	0.16±0.03
	FR43-1	Pyrite	37.15	15.48	24.00±1.76	1.72±0.13
	FR43-5-2	Arsenopyrite	9.8	7.37	13.30±2.20	0.96±0.16
Goutouling	GTL55-2-1	Pyrite	1.57	5.07	3.10±0.67	0.22±0.05
	GTL55-2-2	Pyrite	9.21	15.09	6.10±1.57	0.44±0.11
Taoxiwo	TXW3-8	Pyrite	1.2	6.06	1.98±0.45	0.14±0.03
	TXW3-14	Pyrite	0.66	3.4	1.95±0.57	0.14±0.04

[a] Rc is the He isotope ratio of the sample, and Ra is the He isotope ratio of the atmosphere (1 Ra = 1.39×10^{-6}).

Table 4
The Pb isotopic composition of sulfides, feldspars and country rock samples from the Furong tin deposit

Rock/mineral	Location	Mineral	$^{208}Pb/^{204}Pb$	$^{207}Pb/^{204}Pb$	$^{206}Pb/^{204}Pb$
Ore minerals	Ore vein 10 of Bailashui	Pyrite	39.563	15.709	19.18
	Ore vein 10 of Bailashui	Pyrite	38.263	15.699	19.076
	Ore vein 10 of Bailashui	Pyrite	38.721	15.825	19.745
	Ore vein 10 of Bailashui	Pyrite	37.98	15.598	18.594
	Ore vein 10 of Bailashui	Pyrite	38.206	15.707	18.745
	Ore vein 10 of Bailashui	Pyrite	38.384	15.742	18.784
	Ore vein 10 of Bailashui	Pyrite	39.058	15.693	18.833
	Ore vein 19 of Bailashui	Chalcopyrite	37.986	15.664	18.593
	Ore vein 19 of Bailashui	Pyrite	38.713	15.656	18.741
	Ore vein 19 of Bailashui	Pyrite	37.962	15.645	18.71
	Ore vein 19 of Bailashui	Arsenopyrite	38.768	15.671	18.623
	Ore vein 19 of Bailashui	Chalcopyrite	37.912	15.64	18.569
	Ore vein 19 of Bailashui	Pyrite	37.957	15.651	18.547
	Ore vein 19 of Bailashui	Pyrite	38.132	15.73	18.643
	Ore vein 19 of Bailashui	Chalcopyrite	37.953	15.663	18.629
	Ore vein 19 of Bailashui	Arsenopyrite	38.038	15.68	18.645
	Ore vein 19 of Bailashui	Arsenopyrite	37.941	15.645	18.659
	Ore vein 19 of Bailashui	Sphalerite	38.209	15.733	18.641
	Ore vein 19 of Bailashui	Sphalerite	38.414	15.799	18.714
	Ore vein 55 of Goutongling	Pyrite	38.187	15.724	18.686
	Ore vein 55 of Goutongling	Galenite	38.029	15.685	18.616
	Ore vein 55 of Goutongling	Pyrite	38.011	15.671	18.623
	Ore vein 55 of Goutongling	Pyrite	38.884	15.718	18.648
	Ore vein 3 of Taoxiwo	Pyrite	38.752	15.662	18.589
	Ore vein 3 of Taoxiwo	Arsenopyrite	38.162	15.719	18.657
	Ore vein 3 of Taoxiwo	Pyrite	38.811	15.693	18.621
	Ore vein 3 of Taoxiwo	Pyrite	38.965	15.743	18.658
	Ore vein 3 of Taoxiwo	Arsenopyrite	38.95	15.734	18.655
	Ore vein 3 of Taoxiwo	Arsenopyrite	38.039	15.679	18.615
Granite	Lijiadong unit	Feldspar	39.048	15.697	18.836
	Lijiadong unit	Feldspar	38.961	15.699	18.769
	Lijiadong unit	Feldspar	39.007	15.685	18.815
	Lijiadong unit	Feldspar	38.526	15.503	18.543
	Lijiadong unit	Feldspar	39.099	15.772	18.819
	Nanxi unit	Feldspar	38.875	15.694	18.675
	Nanxi unit	Feldspar	38.997	15.742	18.737
	Nanxi unit	Feldspar	38.976	15.732	18.71
	Nanxi unit	Feldspar	38.925	15.707	18.682
	Nanxi unit	Feldspar	38.916	15.706	18.685
	Jiangjunzhai unit	K-feldspar	38.799	15.68	18.673
	Jiangjunzhai unit	K-feldspar	38.829	15.693	18.664
	Jiangjunzhai unit	K-feldspar	38.823	15.664	18.654
	Jiangjunzhai unit	Feldspar	38.607	15.632	18.467
	Jiangjunzhai unit	Feldspar	38.932	15.713	18.738
	Wuliqiao unit	Feldspar	38.861	15.698	18.63
	Wuliqiao unit	Feldspar	38.905	15.713	18.723
	Wuliqiao unit	Feldspar	38.767	15.647	18.651
	Wuliqiao unit	Feldspar	38.811	15.686	18.653
	Wuliqiao unit	Feldspar	38.829	15.694	18.661
Wall rock		Marble	39.106	15.738	20.121
		Marble	39.284	15.729	20.42

$^{208}Pb/^{204}Pb = 38.607 \sim 39.099$. However, the Pb isotopic composition of the two marbles from the contact zone is heavier than that of the sulfides or feldspars.

The $\delta^{34}S$ values of sulfides from the Furong deposit vary widely from −26.1‰ to +10.4‰, a difference of 36.5‰. Sulfides from the Bailashui ore zone have $\delta^{34}S$ values ranging from −24.4‰ to +10.4‰; values from the Taoxiwo and Shanmenkou ore zones are positive, whereas those from the Goutouling ore zone are negative.

5. Discussion

The Furong tin deposit is located within the A-type Qitianling granite complex and along its contact with the wall rocks. The main period of tin mineralization was contemporaneous with intrusion of the Qitianling granite, implying a temporal and spatial link between the deposit and the granite. In the following paragraphs, we discuss three aspects of this relationship.

5.1. He isotopic composition and its geological implication

Helium in fluid inclusions of the Furong samples may have been affected by late diffusion-induced loss, xenogenous superposition and isotope fractionation. The authors studied the influence of these post-entrapment processes on He isotopic compositions and concluded that the measured $^3He/^4He$ ratios in the Furong sulfide sample represent the initial $^3He/^4He$ ratios of the ore-forming fluids (Li et al., 2006). It is possible that the measured ratios represent the average composition of fluids of several generations, however, the pyrite and arsenopyrite grains have perfect crystal forms, and fluid inclusions in syngenetic quartz and fluorite are dominated by isolated V-L fluid inclusions. Both of these observations suggest that the pyrite and arsenopyrite formed during a single mineralizing event and where not modified by later processes. We conclude that most of the fluid inclusions in sulfides are primary, and that the measured $^3He/^4He$ ratios reflect the compositions of the ore-forming fluids.

Turner et al. (1993) proposed that noble gases in crustal fluids are derived from three sources; air-saturated rainwater, the mantle and the crust. Because the He content of the atmosphere is too low to affect He abundances and isotopic compositions of crustal fluids (Marty et al., 1989; Stuart et al., 1994), the helium in the fluid inclusions from the Furong deposit must have been derived primarily from the mantle and crust. Characteristic $^3He/^4He$ ratios of crustal rocks are 0.01–0.05 Ra (Stuart et al., 1995), whereas those of the mantle are 6–7 Ra (Dunaim and Baur, 1995). The measured $^3He/^4He$ ratios in the Furong deposit range from 0.13 to 2.95 Ra, higher than those of the crust, but lower than those of the mantle. These values suggest that most of the He in these inclusions was derived from the crust, with only a small input from the mantle. This interpretation is confirmed by Fig. 6, which shows that the $^3He/^4He$ ratios of the Furong ore-forming fluids are all within the range of 10^{-5}–10^{-7}, intermediate between the mantle and the crust, although there are some differences among the three studied ore zones. These variations may reflect involvement, in different proportions, of surface-derived fluids in the mineralization. For example, samples FR-19-14 and FR-19-15, which have relatively low $^3He/^4He$ ratios, are from the F30 fault zone, a zone in which there may have been significant involvement of surface-derived fluids in the mineralization process.

The Qitianling granite complex is an A-type granite emplaced in a post-orogenic extensional setting (Zheng and Jia, 2001), related to mantle upwelling and crustal extension. In such an environment, mantle material would have been involved in magma generation (Huang et al., 2001), and both the Qitianling complex and Furong deposit show evidence of a mixed crust-mantle origin. A close temporal and spatial relationship between the two (Wang et al., 2004) is suggested by such features in the granite as: 1) wide variations in texture and structure, and many disequilibrium textures; 2) extensive high temperature alteration and metasomatism,

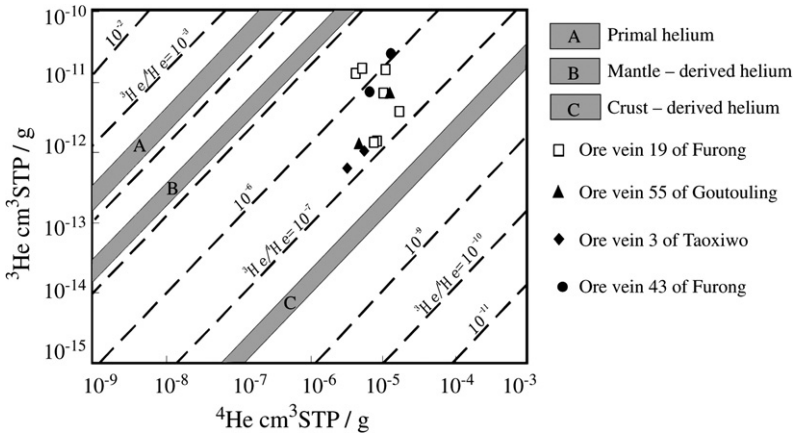

Fig. 6. Helium isotopic composition and evolution of the Furong tin deposit (A, B, C after Mamyin and Tolstikhin, 1984).

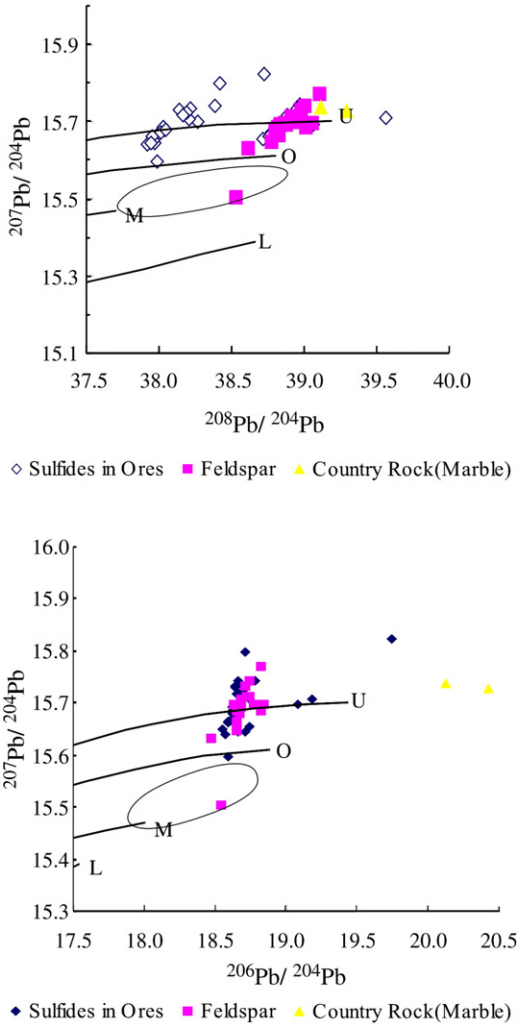

Fig. 7. Lead isotope compositions ($^{207}Pb/^{204}Pb$ versus $^{208}Pb/^{204}Pb$ and $^{207}Pb/^{204}Pb$ versus $^{206}Pb/^{204}Pb$) of samples from the Furong tin deposit and the Qitianling granite complex plotted in the model lead evolution diagrams of Zartman and Doe (1981). M, upper mantle-source lead; L, lower crust-source lead; O, orogenic belt-source lead; U, supracrustal-source lead.

accompanied by albitization and the growth of K-feldspar; and 3) the presence of abundant melt and fluid inclusions in quartz grains. The mineralizing fluids in the deposit must have been closely associated with emplacement of the Qitianling granite and the mixing of mantle and crustal helium reflects crustal melting produced by upwelling of mantle-derived magma.

5.2. Pb isotopic composition and its geological implication

On the basis of 300 lead isotope analyses of 30 stratabound deposits in China, Chen (1981) suggested that the lead can be divided into three types; ordinary, anomalous and mixed. Lead in the sulfides and feldspars of the Furong deposit (Table 4) corresponds to the ordinary variety. The lead isotope compositions of sulfides, feldspars and wall rocks are plotted in the lead isotope evolution diagrams of Zartman and Doe (1981) in Fig. 7. Both the sulfide minerals and feldspars from the four ore zones lie mostly along the supracrustal lead evolution curve, except for two samples, one of which is close to the orogenic evolution curve and the other in the mantle field (Fig. 7). These data indicate that the Pb was derived mostly from the upper crust, with a very minor mantle or lower crustal component. However, the Pb isotope characteristics of the sulfides and feldspars are significantly different from the marbles that host the Qitianling complex, indicating a different source. The Pb in the sulfide minerals and feldspars probably came mostly from the magma, and probably represents mixtures of subduction zone lead and supracrustal or mantle lead (Fig. 8). However, it is surprising that the sulfide samples and feldspars plot in different parts of the mixed field (Fig. 8). This may be due to the accumulation of radiogenic lead from decay of radioactive isotopes in the feldspars.

5.3. S isotopic composition and its geological implication

The $\delta^{34}S$ values of sulfides from the Furong deposit vary widely from +10.4‰ to 26.1‰ (Fig. 9A), with the greatest range in the Bailashui zone (−24.5‰ to +10.4‰) (Fig. 9B). This wide range of isotopic values

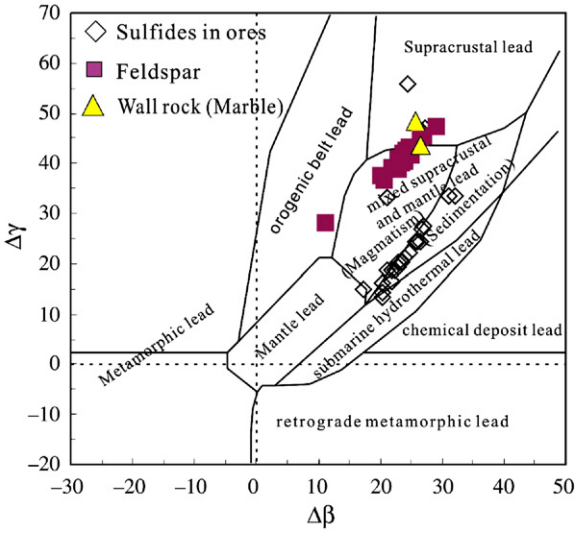

Fig. 8. Δγ–Δβ diagram of ore lead from the Furong tin deposit (Zhu, 1998).

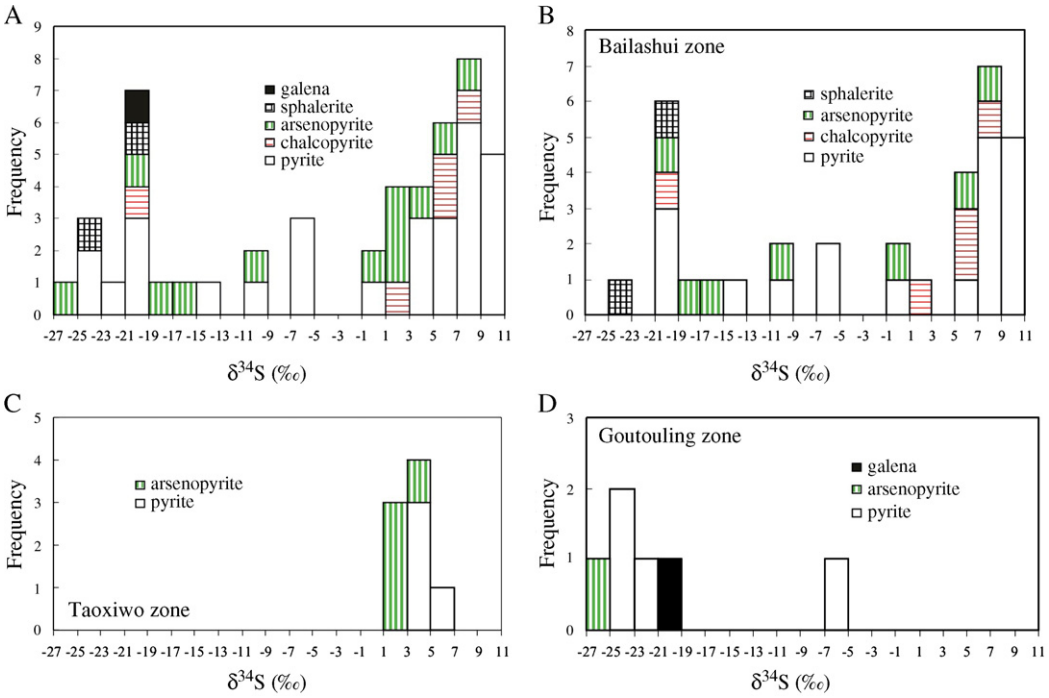

Fig. 9. Composite sulfur isotopic composition histogram of the Furong tin deposit and histograms for each zone.

from the Bailashui zone indicate simultaneous incorporation of heavy and light sulfur in the hydrothermal fluids from which the ores were deposited. The Shanmenkou and Taoxiwo (Fig. 9C) zones have relatively homogeneous isotopic values (+1.7‰ to +7.0‰), indicating a much greater contribution from the magma to the hydrothermal fluids. Values from the Goutouling zone (Fig. 9D) are strongly negative (−20.9‰ to −26.1‰ (except for one sample), indicating much higher enrichment of biogenic sulfur which may derive from the crustal hydrothermal fluids. Sulfur isotope patterns among the different zones are similar to those of the He isotopes in sulfide minerals. These isotopic patterns may reflect the different types of mineralization in the different zones, e.g., altered structural-skarn ores in the Bailashui, skarn ores in the Goutouling zone and greisen ores in the Taoxiwo zone. The isotope data indicate that the sulfur in these zones came from different sources (Table 5).

Of the 49 sulfides analysed from the deposit, 29 have $\delta^{34}S$ values between +0.2‰ and +10.4‰, with an average of +5.9‰. This observation, coupled with the association of the Furong deposit with the Qitianling granite complex suggests that the ore-forming fluids were mainly magmatic related to the granite intrusion. The high positive $\delta^{34}S$ values indicate enrichment of heavy sulfur isotopes derived from the host sedimentary rocks, whereas the low positive values of two samples (+0.2‰ and +0.9‰) are characteristic of mantle sulfur. The high negative $\delta^{34}S$ values indicate enrichment of light biogenic sulfur isotopes.

6. Conclusions

(1) The He isotopic compositions of the Furong tin deposit reflect mixing of mantle-derived and crust-derived He, and the mixing occurred mainly during emplacement of the Qitianling granite complex.

(2) The Pb isotopic composition of sulfides and feldspars from the Furong deposit and the Qitianling granite are similar and their Pb was derived mainly from the upper crust, with a minor mantle or orogenic belt contribution. The Pb in the ores probably came mostly from the Qitianling granite magma.

(3) The S isotopic compositions of the Furong deposit indicate that the ore-forming fluids were derived predominantly from magmatic fluids associated with the Qitianling granite complex, with minor contributions from mantle-derived sulfur, sedimentary sulfur and biogenic sulfur.

(4) The temporal and spatial association of the Furong deposit and the Qitianling granite, coupled

Table 5
The S isotopic composition of sulfides from the Furong tin deposit

Zone	Sample no.	Location	Mineral	δ34SVCDT
Bailashui	FR2-10-1	Ore vein 10 of Bailashui	Pyrite	−5.4
	FR2-10-3	Ore vein 10 of Bailashui	Pyrite	7.5
	FR2-10-5	Ore vein 10 of Bailashui	Pyrite	5.9
	FR2-10-8	Ore vein 10 of Bailashui	Pyrite	10.4
	FR2-10-9	Ore vein 10 of Bailashui	Pyrite	9
	FR2-10-10	Ore vein 10 of Bailashui	Pyrite	9.3
	YJC-1	Ore vein 10 of Bailashui	Pyrite	10.3
	FR3-10-1	Ore vein 10 of Bailashui	Pyrite	−9.8
	FR3-10-3	Ore vein 10 of Bailashui	Pyrite	0.9
	TPK2-23	Ore vein 19 of Bailashui	Pyrite	8.2
	TPK2-28	Ore vein 19 of Bailashui	Chalcopyrite	8.1
	WCP2-18	Ore vein 19 of Bailashui	Pyrite	−6.5
	WCP2-22	Ore vein 19 of Bailashui	Arsenopyrite	−16.8
	WCP2-23	Ore vein 19 of Bailashui	Pyrite	−20.7
	WCP2-25	Ore vein 19 of Bailashui	Pyrite	−14.2
	WCP2-26	Ore vein 19 of Bailashui	Arsenopyrite	−17.1
	WCP2-29	Ore vein 19 of Bailashui	Pyrite	−20
	WCP2-31	Ore vein 19 of Bailashui	Chalcopyrite	−20.6
	WCP2-32	Ore vein 19 of Bailashui	Pyrite	−19.9
	WCP2-33-1	Ore vein 19 of Bailashui	Arsenopyrite	−11
	WCP3-1	Ore vein 19 of Bailashui	Chalcopyrite	5.4
	WCP3-3	Ore vein 19 of Bailashui	Pyrite	8.2
	WCP3-5	Ore vein 19 of Bailashui	Pyrite	8.4
	WCP3-6	Ore vein 19 of Bailashui	Pyrite	8.3
	WCP3-7	Ore vein 19 of Bailashui	Pyrite	9.2
	WCP3-8	Ore vein 19 of Bailashui	Chalcopyrite	2.9
	WCP3-10	Ore vein 19 of Bailashui	Arsenopyrite	−19.8
	FR3-19-2	Ore vein 19 of Bailashui	Sphalerite	−20.8
	FR3-19-3	Ore vein 19 of Bailashui	Sphalerite	−24.5
	FR-43-1	Ore vein 43 of Bailashui	Arsenopyrite	0.2
	FR-43-2	Ore vein 43 of Bailashui	Arsenopyrite	6
	FR-43-5-2	Ore vein 43 of Bailashui	Arsenopyrite	8
	FR-43-7-2	Ore vein 43 of Bailashui	Chalcopyrite	6.7
Shanmenkou	SMK-54-2	Ore vein 54 of Shanmenhou	Pyrite	7
	SMK-54-4	Ore vein 54 of Shanmenkou	Pyrite	6.2
Goutouling	GTL2-1	Ore vein 55 of Goutouling	Pyrite	−21.6
	GTL2-3	Ore vein 55 of Goutouling	Galenite	−20.9
	GTL2-4	Ore vein 55 of Goutouling	Pyrite	−24.4
	GTL2-21-2	Ore vein 55 of Goutouling	Pyrite	−5.4
	GTL2-27	Ore vein 55 of Goutouling	Pyrite	−24.3
	GTL2-27	Ore vein 55 of Goutouling	Arsenopyrite	−26.1
Taoxiwo	TXW2-2	Ore vein 3 of Taoxiwo	Arsenopyrite	2.4
	TXW2-3-1	Ore vein 3 of Taoxiwo	Pyrite	5.2
	TXW2-4	Ore vein 3 of Taoxiwo	Pyrite	3.7
	TXW2-6-1	Ore vein 3 of Taoxiwo	Arsenopyrite	1.9
	TXW2-8	Ore vein 3 of Taoxiwo	Pyrite	4.8
	TXW2-9	Ore vein 3 of Taoxiwo	Pyrite	3.6
	TXW2-9	Ore vein 3 of Taoxiwo	Arsenopyrite	1.7
	TXW2-13	Ore vein 3 of Taoxiwo	Arsenopyrite	3.5

with the He, Pb and S isotopic data, demonstrate that mixing of mantle and crustal material occurred during emplacement of the Qitianling granite. Upwelling of parental mantle melts led to mixing of mantle and crustal materials during extension of the lithosphere in South China in the Mesozoic. The Furong deposit was formed from hydrothermal fluids fractionated from magma that produced the Qitianling granite. Multi-stage deposition reflects episodic cooling of the granite and the development of faults in the pluton and the wall rock.

Acknowledgments

We are most grateful to Prof. Carol D. Frost for her useful suggestions for improving the manuscript. The comments and advice of two anonymous reviewers were also helpful in producing a revised version of the manuscript. Special thanks go to the staff of the South Hunan Institute of Mineral Resources and Survey for their hospitality during the fieldwork. Prof. Paul Robinson is thanked for his careful revision in expression and organization of the manuscript. This research was supported jointly by the Knowledge-innovation Program of the Chinese Academy of Sciences (KZCX3-SW-125) and the National Natural Science Foundation of China (40373020).

References

Ballentine, C.J., Burgess, R., Marty, B., 2002. Tracing fluid origin, transport and interaction in the crust. Reviews in Mineralogy and Geochemistry 47, 539–614.

Bi, C.S., Shen, X.Y., Xu, Q.S., 1992. A new discovery of tin deposit related to Hercynian A-type granite in China. Science in China. Series B, Chemistry, Life Sciences & Earth Sciences 22, 632–638 (in Chinese with English abstract).

Burnard, P.G., Polya, D.A., 2004. Importance of mantle-derived fluids during granite associated hydrothermal circulation: He and Ar isotopes of ore minerals from Panasqueira. Geochimica et Cosmochimica Acta 68, 1607–1615.

Burnard, P.G., Hu, R., Turner, G., Bi, X., 1999. Mantle, crustal and atmospheric noble gases in Ailaoshan gold deposits, Yunnan Province, China. Geochimica et Cosmochimica Acta 63, 1595–1604.

Cai, J.H., Wei, C.S., Sun, M.H., Wei, S.L., Huang, G.F., 2004. Genetic study about the Bailashui tin deposits in Qitianling area of Hunan. Geotectonica et Metallogenia 28, 45–52 (in Chinese with English abstract).

Chen, H.S., 1981. Lead isotopic characteristics in the stratabound ore deposits. Chinese Science Bulletin 10, 612–616 (in Chinese with English abstract).

Chen, Y.C., Mao, J.W., 1995. Mineral Deposit Series and Metallogenical Evolution Traces of Northern Guangxi Province. Guangxi Science and Techndogy Publishing House Press, Nanning, pp. 48–128 (in Chinese with English abstract).

Collins, W.J., Beams, S.D., White, A.J.R., 1982. Nature and origin of A-type granites with particular reference to southeastern Australia. Contributions to Mineralogy and Petrology 80, 189–200.

Deng, J.F., Mo, X.X., Zhao, H.L., Wu, Z.X., Luo, Z.H., Su, S.G., 2004. A new model for the dynamic evolution of Chinese lithosphere: continental roots-plume tectonics'. Earth-Science Reviews 65, 223–275.

Dunaim, T.J., Baur, H., 1995. Helium, neon and argon systematics of the European subcontinental mantle: implications for its geochemical evolution. Geochimica et Cosmochimica Acta 59, 2767–2783.

Eby, G.N., 1992. Chemical subdivision of the A-type granitoids: Petrogenises and tectonic implication. Geology 20, 641–644.

Haapala, I., 1995. Metallogeny of the rapakivi granites. Mineralogy and Petrology 54, 149–160.

Hu, R., Burnard, P.G., Turner, G., Xianwu, B., 1998. Helium and argon isotope systematics in fluid inclusions of Machangqing copper deposit in West Yunnan Province, China. Chemical Geology 146, 55–63.

Huang, J.Q., 1960. Summary on the basic features of tectonics in China. Acta Geologica Sinica 40, 1–37.

Huang, G.F., Zeng, Q.W., Wei, S.L., Xu, Y.M., Hou, M.S., Kang, W.Q., 2001. Geological characteristics and ore-controlling factors of the Furong deposit, Qitianling, Hunan. Chinese Geology 28, 30–34 (in Chinese with English abstract).

Janecka, J., Stemprok, M., 1967. Endogenous tin mineralization in the Bohemian massif. A Technical Conference on Tin, London, pp. 245–266.

Kendrick, M.A., Burgess, R., Pattrick, R.A., Turner, G., 2001. Fluid inclusion noble gas and halogen evidence on the origin of Cu-porphyry mineralizing fluids. Geochimica et Cosmochimica Acta 65, 2651–2668.

Kendrick, M.A., Burgess, R., Pattrick, R.A., Turner, G., 2002. Hydrothermal fluid origins in a fluorite-rich Mississippi valley-type district; combined noble gas (He, Ar, Kr) and halogen (Cl, Br, I) analysis of fluid inclusions from the South Pennine ore field, United Kingdom. Economic Geology 97, 435–451.

Lenharo, S.L.R., Pollard, P.J., Born, H., 2003. Petrology and textural evolution of granites associated with tin and rare-metals mineralization at the Pitinga mine, Amazonas, Brazil. Lithos 66, 37–61.

Li, Y.H., Li, J.C., Song, H.B., Guo, L.H., 2002. Helium isotope studies of the mantle xenoliths and megacrysts from the Cenozoic basalts in the eastern China. Science in China (D) 45, 174–183.

Li, Z.L., Hu, R.Z., Peng, J.T., Bi, X.W., Li, X.M., 2006. Helium isotope geochemistry of ore-forming fluids from the Furong tin orefield in Hunan Province, China. Resource Geology 56, 9–15.

Liu, J.Y., Yu, H.X., Wu, G.Q., 1997. Aakali granites and tin deposits of the Kalam aili area, Northern Xingjiang. Geological Exploration for Non-ferrous Metals 6, 129–135 (in Chinese with English abstract).

Liu, Y.M., Xu, J.F., Dai, T.M., Li, X.H., Deng, X.G., Wang, Q., 2003. ^{40}Ar–^{39}Ar isotopic ages of Qitianling granite and their geologic implications. Science in China (D) 46, 50–59.

Mamyin, B.A., Tolstikhin, I.N., 1984. Helium Isotopes in Nature. Elsevier, Amsterdam, p. 273.

Mao, J.W., Li, Y.H., Li, H.Y., Wang, D.H., Song, H.B., 1997. Helium isotopic evidence on metalgenisis of mantle fluids in the Wangu gold deposit, Hunan Province. Geological Review 43, 646–649 (in Chinese with English abstract).

Mao, J.W., Li, X.F., Lehmann, B., 2004. ^{40}Ar–^{39}Ar dating of tin ores and related granite in Furong tin orefield, Hunan Province, and its geodynamic significance. Mineral Deposits 23, 164–175 (in Chinese with English abstract).

Marty, B., Jambon, A., Sano, Y., 1989. Helium isotopes and CO_2 in volcanic gases of Japan. Chemical Geology 76, 25–40.

Nilson, F.B., Márcia, A., 1998. Granite-ore deposit relationships in Central Brazil. Journal of South American Earch Sciences 11, 427–438.

Qu, X.M., Hou, Z.Q., Zhou, S.G., 2002. The age and tectonic setting of Lianlong Sn-bearing granite in western Sichuan Province. Acta Geoscientia Sinica 23, 223–228 (in Chinese with English abstract).

Robb, L.J., Robb, V.H., Walraven, F., 1994. The Albert silver mine revised: toward a model for polymetallic mineralization in granites of the Bushveld complex, South Africa. Exploration and Mining Geology 3, 247–262 (Canadian Insititute of Mining, Metallorgy and petrology).

Sawkins, F.J., 1984. Metal deposits in relation to plate tectonics. Springer-Verlay, p. 315.

Simmons, S.F., Sawkins, F.J., Schlutter, D.J., 1987. Mantle-derived helium in two Peruvian ore deposits. Nature 329, 429–432.

Stuart, F.M., Turner, G., Duckworth, R.C., Fallick, A.E., 1994. Helium isotopes as tracers of trapped hydrothermal fluids in ocean-floor sulfides. Geology 22, 823–826.

Stuart, F.M., Burnard, P.G., Taylor, R.P., Turner, G., 1995. Resolving mantle and crustal contributions to ancient hydrothermal fluids: He–Ar isotopes in fluid inclusions from DaeHwa W–Mo mineralisation, South Korea. Geochimica et Cosmochimica Acta 59, 4663–4673.

Sun, S.S., McDonough, W.F., 1989. Chemical and isotopic systematics of oceanic basalts; implications for mantle composition and processes. In: Saunders, A.D., Norry, M.J. (Eds.), Magmatism in the Ocean Basins. Geological Society of London, London, pp. 313–345.

Taylor, G.R., 1979. Geology of tin deposits. AmAlsevier, New York.

Turner, G., Burnard, P., Ford, J.L., Gilmour, J.D., Lyon, I.C., Stuart, F.M., 1993. Tracing fluid sources and interaction. Philosophical Transactions of the Royal Society of London 344, 127–140.

Wang, X.W., Wang, X.D., Liu, J.Q., Chang, H.L., 2004. Relationship of Qitianling granite to Sn mineralization in Hunan Province. Geological Science and Technology Information 23, 1–12 (in Chinese with English abstract).

Wei, S.L., Zeng, Q.W., Xu, Y.M., 2002. Characteristics and ore prospects of tin deposits in the Qitianling area, Hunan. Chinese Geology 29, 67–75 (in Chinese with English abstract).

Yamamoto, J., Watanabe, M., Nozaki, Y., Sano, Y., 2001. Helium and carbon isotopes in fluorites; implications for mantle carton contribution in an ancient subduction zone. Journal of Volcanology and Geothermal Research 107, 19–26.

Zartman, R.E., Doe, B.R., 1981. Plumbotectonics the model. Tectonophysics 75, 135–162.

Zhao, K., Jiang, S., Xiao, H., Ni, P., 2002. Origin of ore-forming fluids of the Dachang Sn-polymetallic ore deposits; evidence from helium isotopes. Chinese Science Bulletin 47, 1041–1045.

Zheng, J.J., Jia, B.H., 2001. Geological characteristics and related tin polymetallic mineralization of the Qitianling granite complex in southern Hunan province. Geology and Mineral Resources of South China 9, 50–57 (in Chinese with English abstract).

Zheng, Y.C., Wang, S.J., Feng, J.M., Ouyang, Z.Y., Li, X.Y., 2005. Measurement of the complex permittivity of dry rocks and minerals: Application of polythene dilution method and Lichtenecker's mixture formulae. Geophysical Journal International 163, 1195–1202.

Zhu, B.Q., 1998. The theory and practice of isotope system in Geoscience-concurrent discussion of the continental crust and mantle evolvements in China. Science press, Beijing. (in Chinese with English abstract).

Zhu, J.C., Huang, G.F., Zhang, P.H., Li, F.C., Rao, B., 2003. On the emplacement age and material sources for the granites of Cailing superunit, Qitianling pluton, South Hunan Province. Geological Review 49, 245–252 (in Chinese with English abstract).